

## 10. Main Sequence and Brown Dwarfs

Textbook: §10.6, 13.1 (p. 446–451)

### Zero-age main sequence

The zero-age main sequence (ZAMS) is defined as the beginning of the long, stable period of core hydrogen burning during the star’s lifetime. Stars burn up their (primordial) deuterium via  ${}^2\text{D} + \text{p} \rightarrow {}^3\text{He} + \gamma$  before this point, while they are still contracting towards the main sequence (see Fig. 10.1). Also, the *initial* carbon abundance in stars is much larger than the CN-cycle equilibrium value. For stars of solar metallicity of mass  $\gtrsim 1 M_\odot$ , the reactions that convert  ${}^{12}\text{C}$  to  ${}^{14}\text{N}$  (part of the CN-cycle) can supply the star’s total luminosity for a brief period at the start of hydrogen-burning. This stage is so short that it is often ignored — e.g., it is not shown in the evolutionary tracks of Fig. 10.2 below. In the pre-main-sequence evolutionary tracks of Fig. 7.3, this  ${}^{12}\text{C} \rightarrow {}^{14}\text{N}$  stage causes the last, small upwards-and-downwards wiggle at the end (at left).

### Brown Dwarfs

Stars of masses  $\lesssim 0.08 M_\odot$  do not ignite hydrogen burning in their cores (except possibly for the brief deuterium-burning stage): see the dashed lines in Fig. 10.1. Such stars are known as *brown dwarfs*. A reasonable number of them have been studied, and new spectral classes (e.g., L and T) have been defined to distinguish them via features in their infrared spectra.

### Zero-age main sequence luminosity

For a crude estimate of the luminosity<sup>1</sup>, we use the energy transport equation in terms of mass (Eq. 9.4), and apply it at  $T \simeq \frac{1}{2}T_c$ , where we assume  $L_r \simeq L$  [why?],  $r \simeq \frac{1}{4}R$ , (see Fig. 4.1 for  $n = 3$  and also CO, Fig. 11.4), and take some appropriately averaged opacity  $\bar{\kappa}$ . Furthermore, we approximate  $dT/dM_r \simeq T_c/M$ . Thus,

$$\frac{T_c}{M} \simeq \frac{3}{64\pi^2 ac} \frac{\bar{\kappa} L}{(\frac{1}{4}R)^4 (\frac{1}{2}T_c)^3} \simeq \frac{96}{\pi^2 ac} \frac{\bar{\kappa} L}{R^4 T_c^3} \quad \Rightarrow \quad L \simeq \frac{\pi^2 ac}{96} \frac{R^4 T_c^4}{\bar{\kappa} M}. \quad (10.1)$$

Expressing the central temperature in terms of the central pressure and density using the ideal gas law, and using the expressions for  $P_c$  and  $\rho_c$  appropriate for a polytrope with  $n = 3$ ,

$$T_c = \frac{\mu m_{\text{H}}}{k} \frac{P_{c,\text{gas}}}{\rho_c} = 1.95 \cdot 10^7 \text{ K } \mu \beta \left( \frac{M}{M_\odot} \right) \left( \frac{R}{R_\odot} \right)^{-1}, \quad (10.2)$$

where  $\beta$  was defined as the ratio of the gas pressure and the total pressure. Inserting this in Eq. 10.1,

$$\frac{L}{L_\odot} \simeq 10 \frac{\mu^4 \beta^4}{\bar{\kappa}} \left( \frac{M}{M_\odot} \right)^3. \quad (10.3)$$

### Hot zero-age main-sequence stars

For a hot star, electron scattering dominates in the interior. Thus,  $\bar{\kappa} \simeq 0.2(1 + X) \text{ cm}^2 \text{ g}^{-1}$  (Eq. 5.10). For a star with solar abundances which has just arrived on the main sequence,  $\mu \simeq 0.613$ ,

<sup>1</sup> See KW, chapter 20, for somewhat less crude approximations.

**Table 10.1.** Fractional sizes of the convective core in main-sequence stars

$M_*$ ( $M_\odot$ )	..... ZAMS .....				..... TAMS .....			
	$\log L$ ( $L_\odot$ )	$\log T_{\text{eff}}$ (K)	$M_{\text{cc}}$ ( $M_\odot$ )	$M_{\text{cc}}/M$	$t$ (yr)	$M_*$ ( $M_\odot$ )	$M_{\text{cc}}$ ( $M_\odot$ )	$M_{\text{cc}}/M$
120	6.254	4.739	102.4	0.853	$2.9 \cdot 10^6$	80.9	63.6	0.786
60	5.731	4.693	46.3	0.772	$3.7 \cdot 10^6$	43.0	27.5	0.640
20	4.643	4.552	10.8	0.540	$8.8 \cdot 10^6$	19.1	6.5	0.339
5	2.720	4.244	1.52	0.304	$9.9 \cdot 10^7$	5	0.39	0.078
2	1.177	3.952	0.46	0.229	$1.7 \cdot 10^9$	2	0.13	0.065
1	-0.207	3.732	0	0	$9.7 \cdot 10^9$	1	0	0

and  $L \simeq 4 L_\odot (M/M_\odot)^3$ . For intermediate-mass stars, this estimate agrees reasonably well with detailed models (see Fig. 10.2). The slope, however ( $L \propto M^3$ ) is slightly too shallow between 2 and  $8 M_\odot$ , where the detailed models give  $L \propto M^{3.7}$ ; above  $8 M_\odot$  it is too steep. These effects are due to the presence of a central convection zone and the contribution of radiation pressure. The convection zone increases in size with increasing mass (see Fig. 10.3 and Table 10.1).

### Cool zero-age main-sequence stars

For stars with  $M \lesssim 1 M_\odot$ , the opacity is dominated by bound-free processes. Inserting the estimate Eq. 5.16 in Eq. 10.3, and using  $\rho \simeq \frac{1}{8} \rho_c \simeq 7 \bar{\rho}$  (for an  $n = 3$  polytrope) as well as Eq. 10.2,

$$\frac{L}{L_\odot} \simeq 0.07 \frac{\mu^{7.5}}{Z(1+X)} \left(\frac{M}{M_\odot}\right)^{5.5} \left(\frac{R}{R_\odot}\right)^{-0.5}. \quad (10.4)$$

Thus, given that  $R$  depends approximately linearly on  $M$ , we find a very steep mass-luminosity relation, much steeper than that observed or inferred from models. Furthermore, the luminosity of the Sun is underestimated ( $L \simeq 0.05 L_\odot$  for  $\mu = 0.613$ ,  $Z = 0.02$ ,  $X = 0.708$ ). The reason this does not work as well as for the massive stars, is that with decreasing mass, more and more of the outer region becomes convective; see Fig. 10.3. Only  $\sim 2\%$  of the Sun's mass is convective (although this is nearly the outer  $\sim 30\%$  of the Sun's radius), so a  $n = 3$  polytrope is not completely unreasonable, but stars of  $M \lesssim 0.2 M_\odot$  are completely convective (so a  $n = 1.5$  polytrope would be more appropriate). Furthermore, for very low masses, degeneracy becomes important.

### Evolution on the main sequence

For both hot and cool stars, the luminosity scales with a high power of the mean molecular weight. As hydrogen is burnt,  $\mu$  increases, and therefore the luminosity will increase as well, as can be seen in Fig. 10.2. Numbers for parameters at the beginning and end of the main sequence for massive stars are given in Table 10.1.

### For next time

- Make sure you understand *why* the slopes from the simple estimates are somewhat different from those from detailed models.
- Read about the end of the main sequence: remainder of §13.1.

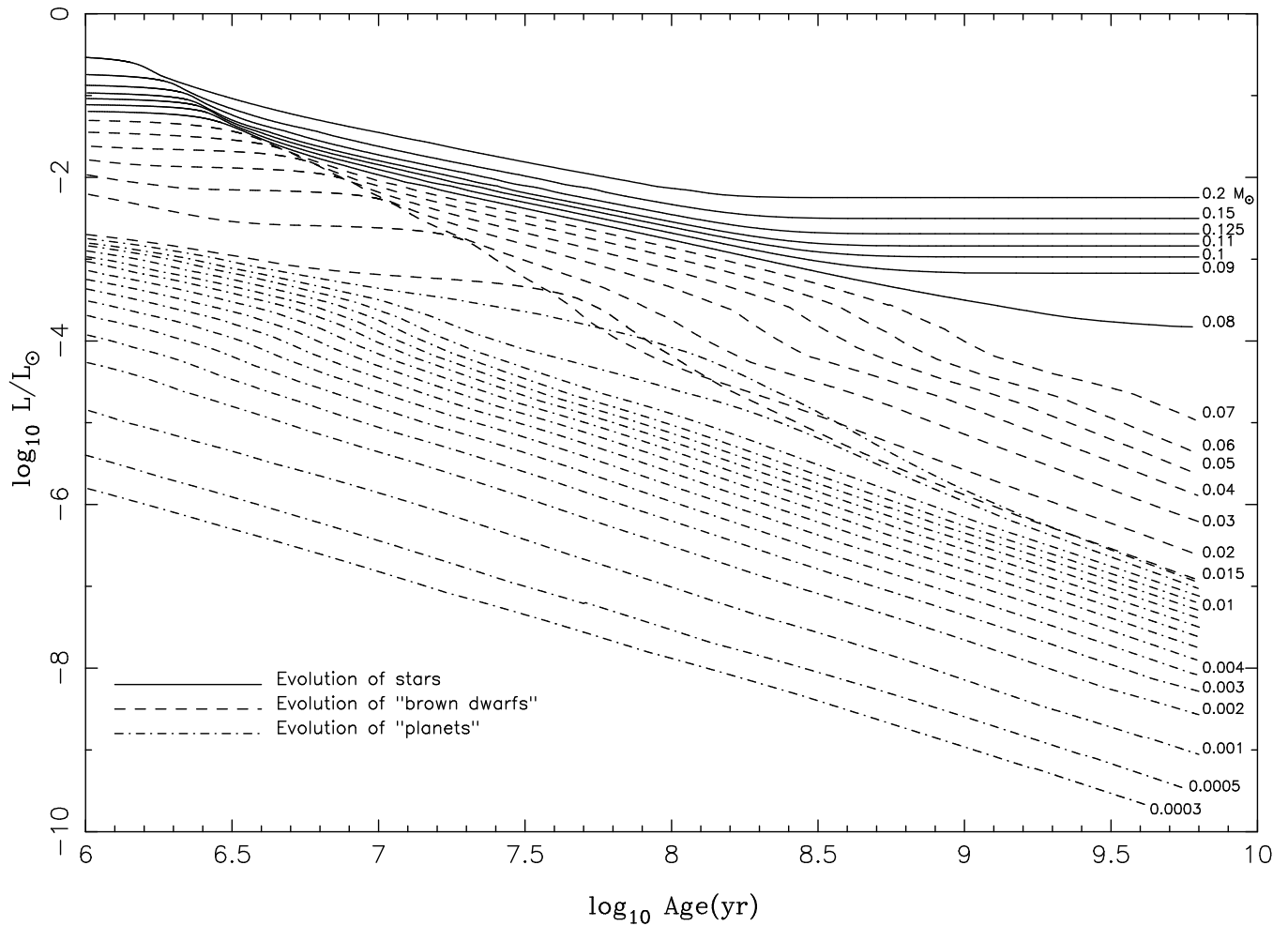


**Fig. 10.1.** Luminosity as a function of time for very low mass stars (*solid lines*) and brown dwarfs (*dashed lines*). The horizontal plateaus in the tracks at upper left show where the period of deuterium burning halts the pre-main-sequence luminosity decline (for a period of up to a few million years) in very low mass stars, as well as in brown dwarfs. Brown dwarfs models of mass  $< 0.015 M_{\odot}$  (i.e., less than about 15 Jupiter masses) have been designated as “planets” (*dot-dashed lines*) in this figure.

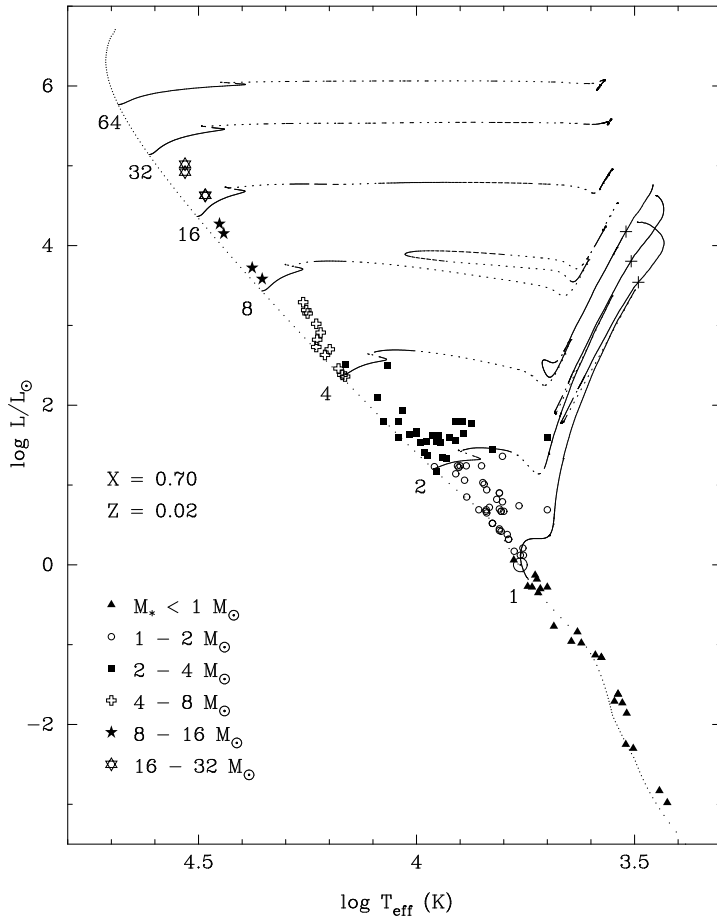


**Fig. 10.2.** HRD for the ZAMS and several evolutionary tracks, calculated with the Eggleton evolutionary code. The labels are masses in solar units. The symbols indicate components of binaries for which the masses, radii, and luminosities were determined observationally. For the tracks, the solid, dotted, and dashed portions indicate where evolution is on a nuclear, thermal, and intermediate time scale, respectively (evolution is upwards and rightwards from the ZAMS; the brief initial  $^{12}\text{C} \rightarrow ^{14}\text{N}$  stage is not shown). For masses  $\geq 2 M_{\odot}$ , the end of the main sequence occurs at the first wiggle in the tracks, a bit to the right of the ZAMS. From Pols et al. (1995, MNRAS 274, 964).

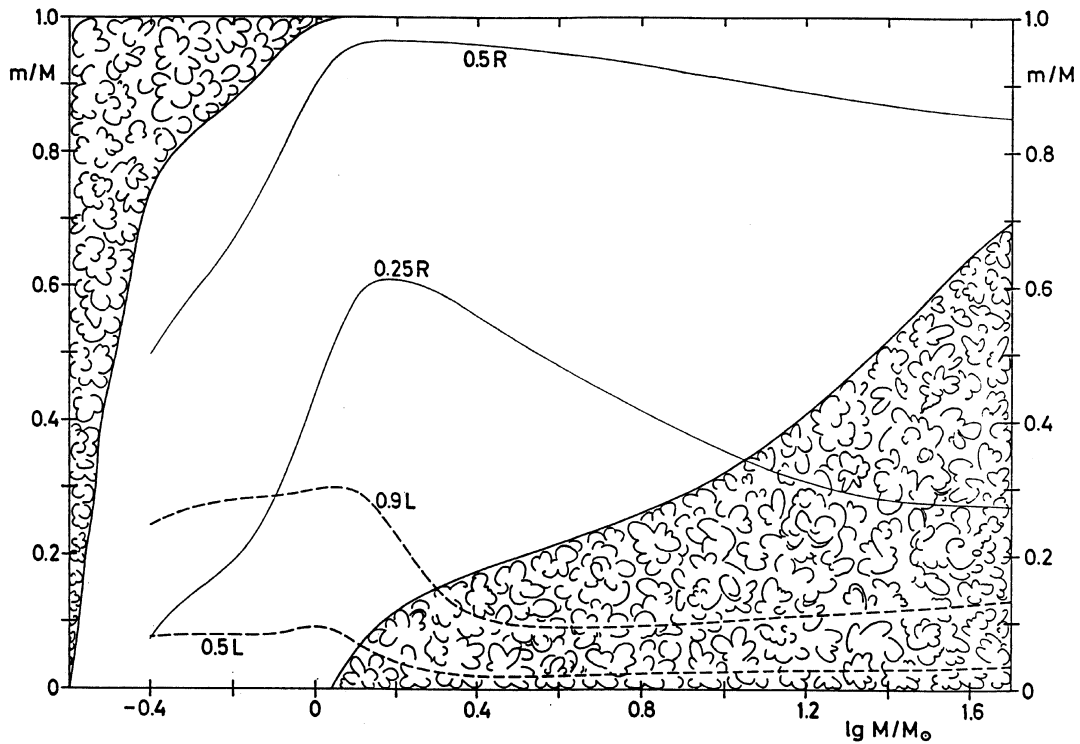


**Fig. 10.3.** Mass fraction  $m/M \equiv M_r/M$  as a function of stellar mass  $M$  at the ZAMS. Convective regions are indicated with the curls. The solid lines indicate the fractional masses at which  $r/R = 0.25$  and  $0.5$ , and the dashed ones those at which  $L_r/L = 0.5$  and  $0.9$ . Taken from KW (their Fig. 22.7).

## 11. The end of the main sequence

Textbook: §13.1, p. 451ff

### *Hydrogen exhaustion in the core*

For more massive stars, hydrogen exhaustion will happen in a larger region at the same time, while for less massive stars, it will initially just be the centre itself. Since in the core one gets  $L_r = 0$ , also the temperature gradient  $dT/dr = 0$ , i.e., the core will become isothermal.

From our discussion of polytropes, it was clear that completely isothermal stars cannot exist ( $\gamma = 1$  and  $n = \infty$ ), but is it possible to have an isothermal core? In the context of polytropes, one could rephrase this as the requirement that averaged over the whole star one has  $\bar{\gamma} > 1.2$  ( $\bar{n} < 5$ ). The result is that for a star in hydrostatic equilibrium, only a relatively small fraction of its mass can be in an isothermal core.

### *Schönberg-Chandrasekhar limit*

For the isothermal core, one can rederive the virial theorem for the case that the pressure external to the object under consideration is not equal to zero. One finds

$$2U_{\text{core}} = -\Omega_{\text{core}} + 4\pi R_{\text{core}}^3 P_{\text{core}}, \quad (11.1)$$

where  $P_{\text{core}}$  is the pressure at the outer boundary of the core.

For an isothermal core (and ideal gas), the internal energy is simply  $U_{\text{core}} = \frac{3}{2} N_{\text{core}} k T_{\text{core}}$ , with  $N_{\text{core}} = M_{\text{core}}/m_{\text{H}}\mu_{\text{core}}$  the number of particles in the core. Writing  $\Omega_{\text{core}} = -q_{\text{core}} G M_{\text{core}}^2/R_{\text{core}}$ , and solving for  $P_{\text{core}}$ , one finds,

$$P_{\text{core}} = \frac{3}{4\pi} \frac{k T_{\text{core}}}{m_{\text{H}}\mu_{\text{core}}} \frac{M_{\text{core}}}{R_{\text{core}}^3} - \frac{q_{\text{core}}}{4\pi} \frac{G M_{\text{core}}^2}{R_{\text{core}}^4}. \quad (11.2)$$

Thus, the expression contains two competing terms, the thermal pressure ( $\sim \bar{\rho} T_{\text{core}}$ ) and the self-gravity ( $\sim R_{\text{core}} \bar{\rho} \bar{g}$ ). Now consider an isothermal core with fixed mass  $M_{\text{core}}$ . For very low external pressure  $P_{\text{env}}$ , the core can provide a matching  $P_{\text{core}}$  for relatively large radius where the thermal term dominates. For increasing external pressure, the radius has to decrease, but clearly at some point the self-gravity will become important, and it becomes impossible to provide a matching  $P_{\text{core}}$ . This maximum pressure can be determined by taking the derivative of Eq. 11.2 with respect to radius<sup>2</sup>, and setting it equal to zero. One finds,

$$R_{\text{core}} = \frac{4}{9} q_{\text{core}} G M_{\text{core}} \frac{m_{\text{H}}\mu_{\text{core}}}{k T_{\text{core}}} \Rightarrow P_{\text{core,max}} = \frac{3}{16\pi} \left(\frac{9}{4}\right)^3 \left(\frac{k T_{\text{core}}}{m_{\text{H}}\mu_{\text{core}}}\right)^4 \frac{1}{q_{\text{core}}^3 G^3 M_{\text{core}}^2}. \quad (11.3)$$

Thus,  $P_{\text{core,max}} \propto T_{\text{core}}^4/\mu_{\text{core}}^4 M_{\text{core}}^2$ , i.e., the maximum pressure an isothermal core can withstand *decreases* with increasing core mass.

For the pressure exerted by the envelope, generally  $P \approx G M^2/R^4$ ,  $\rho \approx M/R^3$ , and, since also  $P_{\text{env}} = k T_{\text{env}} \rho_{\text{env}}/m_{\text{H}}\mu_{\text{env}}$ ,  $T_{\text{env}} \approx (m_{\text{H}}\mu_{\text{env}}/k)(G M/R)$ . Combining,

$$P_{\text{env}} = C_{\text{env}} \frac{1}{G^3 M^2} \left(\frac{k T_{\text{env}}}{m_{\text{H}}\mu_{\text{env}}}\right)^4, \quad (11.4)$$

<sup>2</sup> In CO, p. 492, the derivative is taken with respect to mass. This is rather illogical.

where  $C_{\text{env}}$  is a constant depending on the precise structure of the envelope.

At the boundary,  $T_{\text{env}} = T_{\text{core}}$  and  $P_{\text{env}} < P_{\text{core,max}}$ , i.e.,

$$C_{\text{env}} \frac{1}{G^3 M^2} \left( \frac{kT_{\text{core}}}{m_{\text{H}} \mu_{\text{env}}} \right)^4 < C_{\text{core}} \left( \frac{kT_{\text{core}}}{m_{\text{H}} \mu_{\text{core}}} \right)^4 \frac{1}{G^3 M_{\text{core}}^2}. \quad (11.5)$$

Inserting numerical values of  $C_{\text{core}}$  and  $C_{\text{env}}$  obtained from more detailed studies, one finds

$$\frac{M_{\text{core}}}{M} \lesssim 0.37 \left( \frac{\mu_{\text{env}}}{\mu_{\text{core}}} \right)^2, \quad (11.6)$$

For a helium core ( $\mu_{\text{core}} \simeq \frac{4}{3}$ ) and an envelope with roughly solar abundances<sup>3</sup> ( $\mu_{\text{env}} \simeq 0.6$ ), one thus finds a limiting fractional mass  $M_{\text{SC}} \simeq 0.08M$ .

### *As a function of mass*

With the above, we can describe what will happen when hydrogen is exhausted in the core,

- For massive stars ( $M \gtrsim 6 M_{\odot}$ ), the convective core at hydrogen exhaustion exceeds 8% of the total mass (see Table 10.1). Thus, an isothermal core cannot form. Instead, the core will contract until helium fusion starts. This happens on a thermal timescale, and causes the star to become a red giant (see next chapter).
- For intermediate-mass stars ( $1.4 \lesssim M \lesssim 6 M_{\odot}$ ), an isothermal core will form once hydrogen is exhausted in the centre. Around this core, hydrogen burning will continue, leading to growth of the core. This phase of the evolution is called the *sub-giant* branch. It will continue until the mass of the core exceeds 8% of the total mass, at which time the core has to contract, and the star becomes a red giant on the thermal timescale, as above. For stars more massive than  $M \gtrsim 2.4 M_{\odot}$ , the contraction will be stopped by the ignition of helium burning, while for lower masses degeneracy sets in.
- For low-mass stars ( $M \lesssim 1.4 M_{\odot}$ ), the isothermal core becomes degenerate before the critical mass fraction is reached, and no rapid phase of contraction occurs. Thus, the star moves to the red-giant branch on the nuclear time scale of the shell around the core.

### *For next time*

- Ensure you understand why stars of different mass behave differently when Hydrogen is exhausted in their cores.

---

<sup>3</sup> In general, some processed material will be present in the envelope as well.

## 12. The various giant branches

Textbook: This supplements (and partly *replaces*) §13.2

### *General considerations*

From observations, we see that stars which have left the main sequence, cluster predominantly near low temperatures, but high luminosity. Thus, their radii are large, i.e., they are giants. From observations of globular clusters, one finds that even low-mass stars can become extremely luminous in this phase (see Fig. 1.2). The two basic questions to be addressed are why stars become so cool, and how they can become so much more luminous than they were on the main sequence. Both properties are reproduced in stellar models, but it is not always simple to point to a specific reason why a star behaves as it does. Indeed, even in the last decade there have been a number of articles with titles like “why stars inflate to and deflate from red giant dimensions” (Renzini et al., 1992, ApJ 400, 280) and, in response, “on why intermediate-mass stars become giants after the exhaustion of hydrogen in their cores” (Iben, 1993, ApJ 415, 767). Out of necessity, therefore, the discussion in this chapter will be somewhat vague. To give a framework, schematic evolutionary tracks for a low-mass ( $1 M_{\odot}$ ), an intermediate-mass ( $5 M_{\odot}$ ), and a high-mass ( $25 M_{\odot}$ ) star are shown in Fig. 12.1. One sees that intermediate-mass stars go through the most contorted track. Therefore, the track for the  $5 M_{\odot}$  case is shown in more detail as well, with the important physical processes in the various phases indicated; since this track was taken from an early (less accurate) computation, more recent evolutionary tracks are shown in Fig. 12.2, plus a schematic  $5 M_{\odot}$  case (Fig. 12.3) and  $1 M_{\odot}$  case (Fig. 12.4) with insets showing schematically the abundance profiles at various stages during the star’s evolution.

Regarding the question of the increase in luminosity seen for giants, it is worthwhile to think back to what determines the luminosity on the main sequence. There, in essence, the luminosity is determined by how quickly the envelope can transfer and radiate energy; the star will contract until nuclear fusion generates a matching amount of energy in the core. The principal difference for a giant is that the burning occurs in a shell, whose properties are not just determined by the envelope above, but also by the core below.

As a star’s envelope expands and it becomes a red giant (approaching the Hayashi track), the convective envelope eventually comprises most of the tenuous envelope. In other words, the base of the convective envelope moves inwards in mass  $M_r$  (though not necessarily in radius), reaching into regions that had been partially processed by nuclear burning on the main sequence (CN-cycle and p-p chain reactions). This processed material is thus mixed throughout the convective envelope to become visible at the star’s surface, a process known as “**first dredge-up**” (this stage is indicated in Figs. 12.3 and 12.4). This yields reduced  $^{12}\text{C}/^{13}\text{C}$  and  $C/N$  ratios at the stellar surface; observations of these ratios in stars during this stage of evolution are in fairly good agreement with what is predicted by computational models.

### *Low mass giants*

For low-mass stars, the contraction of the core after hydrogen exhaustion is stopped by electron degeneracy pressure before the core becomes hot enough for helium ignition. Therefore, the Schönberg-Chandrasekhar limit becomes irrelevant, and the core can grow until something more drastic happens. Since no energy is generated within the core, the temperature in the whole core will equilibrate with that in the surrounding hydrogen-burning shell.

**Table 12.1.** Dependencies of  $\rho$ ,  $T$ ,  $P$ , and  $L$  in a shell on  $M_{\text{core}}$  and  $R_{\text{core}}$ .

case	$\eta$	$\nu$	$\alpha_1$	$\alpha_2$	$\beta_1$	$\beta_2$	$\gamma_1$	$\gamma_2$	$\delta_1$	$\delta_2$
CNO, hot	2	13	-3	2.33	1	-1	-2	1.33	7	-5.33
CNO, cool	2	16	-4	3.33	1	-1	-3	2.33	8	-6.33
triple- $\alpha$	3	22	-4.5	4	1	-1	-3.5	3	8.5	-7

Taken from Refsdal & Weigert (1970, A&A 6, 426). For all cases, it is assumed that electron scattering dominates the opacity (i.e.,  $a = b = 0$ ).

### Shell burning around a degenerate core

In the layers near the dense, concentrated core, the pressure structure is dominated by the strong gravitational attraction of the core rather than by the pressure of the overlying envelope. The core becomes more and more dominant as the star evolves, since the core grows in mass and shrinks in size, while the envelope becomes more and more tenuous.

In the limit that the envelope can be considered weightless, and the shell contains a mass much smaller than that of the core (and provided also that the base of the convective envelope does not actually reach *into* the burning shell — see “hot bottom burning” below), the properties of the shell depend only on the mass  $M_{\text{core}}$  and radius  $R_{\text{core}}$  of the core. This implies that the length scale in the shell will be set by  $R_{\text{core}}$ , i.e., that if one compares models for different  $(M_{\text{core}}, R_{\text{core}})$ , the run of pressure, density, etc., with  $r/R_{\text{core}}$  will be very similar. For instance, if in a given model,  $P/P_{\text{core}} = f(r/R_{\text{core}})$ , where  $P_{\text{core}}$  is the pressure at the bottom of the shell (i.e., the outer boundary of the core) and  $f(r/R_{\text{core}})$  a functional dependence on  $r/R_{\text{core}}$ , one then expects that in another model  $P'/P'_{\text{core}} = f(r'/R'_{\text{core}})$ . This expectation is confirmed by real models (see Fig. 12.5). Refsdal & Weigert (1970, A&A 6, 426) used such assumptions to derive the dependencies of  $\rho(r/R_{\text{core}})$ ,  $T(r/R_{\text{core}})$ ,  $P(r/R_{\text{core}})$ , and  $L_r(r/R_{\text{core}})$  on  $M_{\text{core}}$  and  $R_{\text{core}}$  (see also KW, § 32.2). They assumed the ideal gas law, an opacity law  $\kappa = \kappa_0 P^a T^b$ , and energy production  $\epsilon = \epsilon_0 \rho^{\eta-1} T^\nu$  (via reactions with  $\eta$  reactants, where  $\eta = 2$  except for the  $3\alpha$  reaction), and found

$$\begin{aligned}
 \rho(r/R_{\text{core}}) &\propto M_{\text{core}}^{\alpha_1} R_{\text{core}}^{\alpha_2}, & \alpha_1 &= -\frac{\nu-4+a+b}{\eta+1+a}, & \alpha_2 &= \frac{\nu-6+a+b}{\eta+1+a}, \\
 T(r/R_{\text{core}}) &\propto M_{\text{core}}^{\beta_1} R_{\text{core}}^{\beta_2}, & \beta_1 &= 1, & \beta_2 &= -1, \\
 P(r/R_{\text{core}}) &\propto M_{\text{core}}^{\gamma_1} R_{\text{core}}^{\gamma_2}, & \gamma_1 &= 1 - \frac{\nu-4+a+b}{\eta+1+a}, & \gamma_2 &= -1 + \frac{\nu-6+a+b}{\eta+1+a}, \\
 L_r(r/R_{\text{core}}) &\propto M_{\text{core}}^{\delta_1} R_{\text{core}}^{\delta_2}, & \delta_1 &= \nu - \eta \frac{\nu-4+a+b}{\eta+1+a}, & \delta_2 &= -\nu + 3 + \eta \frac{\nu-6+a+b}{\eta+1+a}.
 \end{aligned} \tag{12.1}$$

One sees that the temperature scales with  $M_{\text{core}}/R_{\text{core}}$  independent of details ( $a, b, n, \nu$ ) of the energy generation process and the opacity law (indeed, the scaling follows directly from hydrostatic equilibrium and the ideal gas law). Thus, for a degenerate core with  $R_{\text{core}} \propto M_{\text{core}}^{-1/3}$ , one expects  $T \propto M_{\text{core}}^{4/3}$ . The implied strong dependence of the luminosity on the core mass is only partly offset by the fact that the pressure and density actually decrease with increasing  $M_{\text{core}}$ . Indeed, from numerical values (see Table 12.1), one sees that one has stellar luminosity  $L \propto M_{\text{core}}^{\sim 9}$  for a shell in which hydrogen is burned via the CNO cycle; this is confirmed by detailed models, which find  $L \propto M_{\text{core}}^{\sim 8}$  on the upper RGB (where the envelope is the most extended).

Thus, we see that the luminosity increases very steeply with increasing core mass. Since the envelope is almost completely convective, and the star is close to the Hayashi line, the effective temperature cannot increase much. In the HR diagram, the star therefore moves almost straight

up, along the so-called *ascending* or **red giant branch** (RGB). As the hydrogen shell burns its way outwards in mass  $M_r$ , the convective envelope retreats ahead of it: deepest first dredge-up occurs not far above the base of the RGB (see Fig. 12.4).

On the upper RGB of low mass stars (*subsequent* to first dredge-up), there is evidence of some further CNO-cycle processing of envelope material, in spite of the fact that the base of the convective envelope is at temperatures far too low for such nuclear processing. This indicates that a slow “extra” mixing mechanism is at work (probably driven by rotation effects), mixing some material between the convective envelope and the hydrogen-burning shell. (This is a similar mechanism to that which causes the main-sequence lithium depletion in stars like the Sun.)

## Evolution of the degenerate core

While the core grows, it remains approximately isothermal, and at the temperature of the shell surrounding it. In principle, the increase in temperature goes towards lifting the degeneracy, but this is more than compensated for by the increase in core density,  $\bar{\rho}_{\text{core}} \propto M_{\text{core}}/R_{\text{core}}^3 \propto M_{\text{core}}^2$ ; see Fig. 3.2.

As one increases the density and temperature, however, the helium ions (which are not degenerate) start approaching each other more and more closely during interactions, and will start to fuse when the core mass increases to  $0.45 M_{\odot}$  (and  $T_{\text{core}} \simeq 10^8$  K). [Verify that you understand why this is independent of the total mass of the star.] The fusion will increase the temperature in the core, but will not reduce the density at first, since the pressure exerted by the ions is small compared to the electron degeneracy pressure. With increasing temperature and constant density, energy generation increases exponentially, until finally the thermal pressure becomes high enough to force the core to expand. By this time, the luminosity from the core has become  $\sim 10^{11} L_{\odot}$ , i.e., roughly equal to that from the entire Galaxy! Unfortunately, it does not seem possible to observe this *helium core flash*: the energy is used to expand the envelope.

From detailed models, it turns out that as the degenerate core grows hotter, in its centre the pressure and temperature are sufficiently high that energy is lost in neutrino creation. As a result, the centre will be slightly cooler, and helium core flash ignition will be in a shell around it. Burning will move inwards as the core is heated (possibly in a succession of mini-core-flashes following the main core flash), until degeneracy is lifted throughout the core.

## After the helium core flash

The evolution *during* the helium flash is not very well understood, but it appears to be followed by a phase of quiet helium burning in a non-degenerate core. This core will still have  $M_{\text{core}} \simeq 0.45 M_{\odot}$ , but its radius will have increased significantly. Thus, one expects that the luminosity contributed by the hydrogen shell will be much smaller,  $\sim 100 L_{\odot}$  (down from  $\sim 1000 L_{\odot}$ ). During this time, the position of the star in the HR diagram depends on its metallicity, which determines the opacity in the envelope as well as the efficiency of energy generation in the CNO cycle (via  $X_{\text{CNO}}$ ). For solar metallicity, stars remains near the Hayashi track, in the so-called *red clump* (see the  $2 M_{\odot}$  track in Fig. 12.2, and the 1 and  $2 M_{\odot}$  tracks in Fig. 10.2). For lower metallicities, stars will move to the *horizontal branch* (see Figs 12.1, 12.4, 1.1 and 1.2). The position on the horizontal branch is determined by the envelope mass as well as the metallicity. Mass loss of order  $0.2 M_{\odot}$  appears to take place between the main sequence and the horizontal branch; possibly there is a mass ejection episode due to the helium core flash (although pure stellar wind mass loss on the RGB has not

been ruled out). Some such low mass stars traverse a region of the HR diagram where their outer envelopes are pulsationally unstable, becoming RR Lyrae variables.

After helium is exhausted in the core, the core, now composed of carbon and oxygen, will become degenerate, and burning will continue in a helium shell. This shell will become brighter as the core mass increases, and the star starts to move up the **asymptotic giant branch** (AGB). During the later phases, the burning in the helium shell becomes unstable, leading to so-called *helium shell flashes*, which will be discussed below. During this phase, the envelope mass is reduced by nuclear burning and mass loss. The latter becomes especially important at very high luminosities, when the envelope becomes pulsationally unstable (becoming, e.g., Mira variables, with large pulsation amplitudes). At that time, a so-called “super-wind” starts. Once the hydrogen-rich envelope has dwindled to  $\lesssim 1\%$  of the total mass, it deflates, and the star moves towards the blue at essentially constant luminosity, burning what little material remains. (After the star has left the AGB, there is a period when its surface is hot enough to yield UV radiation that ionizes the material lost most recently, which is then visible as a glowing “planetary nebula” — a misnomer, since it has nothing to do with planets). The star will be left with roughly  $10^{-2} M_{\odot}$  of helium and  $10^{-4} M_{\odot}$  of hydrogen, around a carbon-oxygen white dwarf. From observations of white dwarfs, one finds masses mostly in the range  $0.55\text{--}0.60 M_{\odot}$ . Apparently, the remainder of the envelope mass of low-mass stars is lost in their latest stages.

### *Intermediate mass giants*

For an intermediate-mass star, after hydrogen is exhausted in the core, burning continues in a thick shell around an isothermal core. This can be seen in Fig. 12.6 (following point C), where the changing interior structure of a  $5 M_{\odot}$  star is shown. This corresponds to the phase between points 4 and 5 in Fig. 12.1. A while after point C, the isothermal core reaches the Schönberg-Chandrasekhar limit, and the star moves rapidly towards the red. During this phase, the surface luminosity drops, but this is mostly because part of the energy generated in the core is used for the expansion of the envelope (see below). The star stabilizes again when helium is ignited in the core, and the envelope has become largely convective (point E in Fig. 12.6, point 7 in Fig. 12.1, point 9 in Fig. 12.3 — *this is the point of deepest first dredge-up in intermediate mass stars*).

At this phase, the core (which initially has mass  $\sim 0.75 M_{\odot}$  in a  $5 M_{\odot}$  star) hardly notices that there is another  $4 M_{\odot}$  of shell and envelope around it, and its structure and luminosity are very similar to what they would have been if the core had been an isolated  $0.75 M_{\odot}$  helium main-sequence star. This reflects the fact that the envelope has become so dilute that it exerts negligible pressure. Like for the low-mass stars, the conditions in the hydrogen-burning shell depend almost completely on the properties of the helium-burning core.

When the helium core evolves, its “effective temperature” will at first, like that of a hydrogen main-sequence star, become slightly lower, and its radius will become slightly bigger. As a result, the hydrogen shell becomes less luminous. Since the shell produces most of the star’s luminosity, the luminosity will drop somewhat (just after point E in Fig. 12.6, between 7 and 8 in Fig. 12.1). The mass of the helium core, however, will increase, and this causes the core to move upward in mass along the helium main-sequence, towards somewhat larger radius and higher temperature. The higher temperature causes an increase in the energy production in the shell, and therewith a rise in the star’s luminosity. This corresponds to the increase in luminosity up to point G seen in Fig. 12.6 (between 9 and 10 in Fig. 12.1). During portions of these “blueward loops” in the HR diagram, intermediate mass stars may also lie in regions of the HR diagram where their outer envelopes are pulsationally unstable, becoming Cepheid variables.

When helium is exhausted in the centre, an isothermal carbon-oxygen core forms, and around it helium is burnt in a thick shell (F to G in Fig. 12.6; 10 to 11 in Fig. 12.1). When the core reaches the Schönberg-Chandrasekhar limit, it will collapse (note that the mass of the carbon-oxygen core should be measured relative to the mass of the helium star). As a result, the helium shell will become much more luminous, the layers above it will expand, and the hydrogen shell will be extinguished (H–K, 13–14; note that the extra loop in the HR diagram shown in Fig. 12.1 between points 11 and 14 is probably spurious, as it does not show up in more recent stellar models such as those in Figs. 10.2 and 12.2). This expansion causes the convective envelope to engulf hydrogen-exhausted material that the hydrogen shell had left behind, in a process known as “**second dredge-up**”. (This occurs near point 15 in Fig. 12.3. *Low mass stars*, where the hydrogen-burning shell is not extinguished, *do not experience second dredge-up.*) The core becomes degenerate, and at first there is only a helium shell around it. As the shell eats outwards, it comes close to the position where second dredge-up has left hydrogen-rich material, and the hydrogen shell is re-ignited.

From here on, the evolution becomes similar to the late evolution of low-mass stars. The helium shell becomes unstable, and near the top of the asymptotic giant branch a super wind sets in, which limits the growth of the degenerate core. When the envelope has become too tenuous, it deflates, the star moves to the blue, and a white dwarf is formed.

### *High mass giants*

For even more massive stars, after hydrogen exhaustion the core contracts immediately to helium ignition. This slows down, but does not stop the star from moving across the HR diagram. For the  $25 M_{\odot}$  star shown in Fig. 12.1, helium is exhausted while the star is only midway over to the red-giant branch. At that point, the core contracts further, and carbon is ignited. After that, things move on very fast, and the star soon explodes as a supernova.

The evolution of these massive stars is complicated greatly by mass loss, even on the main sequence. Due to mass loss, the whole hydrogen-rich envelope may disappear, in which case the star becomes a helium star, and moves to high temperatures in the HR diagram. Indeed, for very massive stars, this is virtually unavoidable, as their luminosity on the way to the red giant branch exceeds the Eddington luminosity, and their envelopes are rapidly blown off. This results in an empty region in the top right of the HR diagram, above and to the right of the *Humphreys-Davidson limit* (see Fig. 1.3). Stars close to this limit indeed are observed to have extremely large and variable mass-loss rates; these are the so-called *luminous blue variables*.

### *Helium shell flashes (also called “thermal pulses”)*

Above, it was mentioned that the helium shell could become unstable. To see how this arises, we do a stability analysis for a thin shell and compare this with a similar analysis for a core (which should be stable). For a core, the mass of the burning region goes as  $m \sim \rho r^3$ , and expansion in reaction to an energy perturbation corresponds to a small increase  $\delta r$ . For a thin shell at radius  $r_0$  and with thickness  $D$ , the mass in the burning region goes as  $m \sim \rho r_0^2 D$ . For a small expansion of the shell, the thickness will increase by  $\delta D$  but  $r_0$  will be approximately constant. The corresponding change in density for the two cases (assuming no change in mass of the burning region) can be written in fractional units as

$$\text{core: } \frac{\delta \rho}{\rho} = -3 \frac{\delta r}{r} \quad \text{shell: } \frac{\delta \rho}{\rho} = -\frac{\delta D}{D} = -\frac{r}{D} \frac{\delta r}{r}. \quad (12.2)$$

In the last equality, we used  $\delta r$  to indicate the change in the outer radius of the shell. Assuming the layers outside the expanding core or shell change homologously with the outer radius, we have for both that  $P \propto r^{-4}$ , or  $\delta P/P \propto -4\delta r/r$ . For an ideal gas, the temperature  $T \propto P/\rho$ , and thus the fractional temperature change is  $\delta T/T = \delta P/P - \delta\rho/\rho$ . Similarly, given an energy generation rate  $\epsilon \propto \rho^\lambda T^\nu$ , the fractional change in energy generation rate is  $\delta\epsilon/\epsilon = \lambda\delta\rho/\rho + \nu\delta T/T$ . For the two cases, these fractional changes can be expressed in terms of the fractional change in radius by

$$\begin{aligned} \text{core: } \quad \frac{\delta T}{T} &= (-4 + 3)\frac{\delta r}{r}, & \text{shell: } \quad \frac{\delta T}{T} &= \left(-4 + \frac{r}{D}\right)\frac{\delta r}{r}, \\ \frac{\delta\epsilon}{\epsilon} &= (-3\lambda + \nu(-4 + 3))\frac{\delta r}{r}, & \frac{\delta\epsilon}{\epsilon} &= \left(-\lambda\frac{r}{D} + \nu\left(-4 + \frac{r}{D}\right)\right)\frac{\delta r}{r}. \end{aligned} \quad (12.3)$$

For the core, we thus see that a small expansion ( $\delta r > 0$ ), leads to a decrease in temperature and energy generation rate ( $\delta T < 0$ ,  $\delta\epsilon < 0$ ), i.e., the burning is stable. However, for a shell with  $D \ll r$  (and  $\nu > \lambda$ ), for a small expansion both  $T$  and  $\epsilon$  actually increase, i.e., *burning in a thin shell is unstable*.

While a shell is eating its way out, it tends to become thinner and thus closer to instability. And indeed the instability also occurs in real and model stars, as can be seen in Fig. 12.7. In the left panel, one sees that at the start of the instability, the density decreases and the temperature increases sharply. As a result, the local luminosity becomes several times the total stellar luminosity. This continues until the shell expands sufficiently (i.e., its thickness is no longer much smaller than the radius). Then it gently settles back, until the instability sets in again.

Note that while the luminosity *in* the shell becomes very high, that *at the top* of the shell does not increase so dramatically. This is because most of the energy is used to expand the shell. Furthermore, as the helium shell expands, the temperature in the hydrogen shell drops, and hydrogen burning is temporarily extinguished. Therefore, the luminosity of the star actually goes down during a shell flash. As on the RGB, for stars where envelope convection does not reach into the hydrogen-burning shell, the star’s (interflash) surface luminosity is determined only by the star’s core mass (and metallicity) — after the first few helium shell flashes, a “universal” **core-mass–luminosity relation** is approached, which is almost linear in the core mass.

In the right-hand panels of Fig. 12.7, one sees that a small convection zone appears during the shell flash. This will distribute processed material all through the region between the hydrogen and helium shells. While the shell flash is occurring, the lower boundary of the outer (envelope) convection zone retreats somewhat, in response to the lower hydrogen shell luminosity, and then descends again. Fig. 12.8 shows a case where “**third dredge-up**” occurs, in which the envelope convection descends below the position of the (extinguished) hydrogen shell into the intershell region, and can thus bring up highly processed material to the surface. Observationally, this leads to the formation of S stars (enriched in “s-process” isotopes, that result from slow neutron irradiation) and carbon stars (where the surface C/O ratio exceeds unity).

Surface carbon enrichment (possibly yielding a carbon star) is fairly straightforward, as the  $3\alpha$  reaction during the earlier helium shell flash has enriched the intershell region with  $^{12}\text{C}$ . Formation of S stars is less simple. The observed s-process isotopes at the surface of low mass S stars (and carbon stars) would have required slow irradiation of iron nuclei by a fairly large number of neutrons (the iron is present in the original stellar composition, part of the metallicity). The  $^{22}\text{Ne}(\alpha, n)$  reaction can produce a few neutrons during the helium shell flash, but not enough — the helium-burning temperature is not high enough for this reaction to be significant. On the other hand, the  $^{13}\text{C}(\alpha, n)$  reaction would occur at lower temperatures, but the CNO-cycle burning leaves behind almost no  $^{13}\text{C}$ . This problem could be solved if, during the third dredge-up, a relatively small amount of hydrogen was mixed downwards into the carbon-rich intershell region

(computational models do not exhibit such behavior, but there are several hard-to-model processes that might yield such a result, e.g., semiconvection, partial convective overshoot, rotation-induced mixing, etc.). As this region heated up again, it would burn up the hydrogen via the  $^{12}\text{C}(p, \gamma)$  reaction, yielding a region with a relatively large  $^{13}\text{C}$  abundance. Later, this region would grow hot enough for the  $^{13}\text{C}(\alpha, n)$  reaction to burn up the  $^{13}\text{C}$  and irradiate the local material with neutrons, yielding s-process isotopes. These would be engulfed by the next flash-driven intershell convective region, which would mix them throughout the intershell region; some would then be mixed to the surface in the following dredge-up episode (see Fig. 12.8).

### *Hot bottom burning*

In stars of mass  $\gtrsim 4 M_{\odot}$ , the base of the convective envelope eventually reaches into the hydrogen-burning shell during the interflash period (“hot bottom burning”). This can result in CNO-cycle processing of the envelope, affecting the envelope CNO isotope ratios. When hot bottom burning occurs, the shell’s properties no longer depend only on the core mass: it is also linked to the surface via the the envelope convection. The star’s luminosity increases significantly above the value that would have been expected from the core-mass–luminosity relation mentioned above.

### *The envelope*

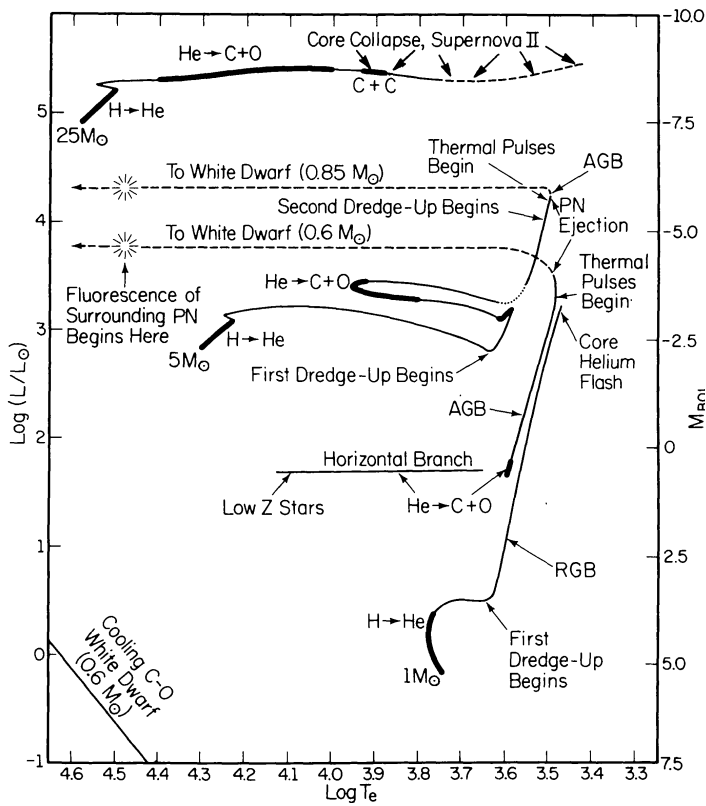
In the above discussion, we have mostly ignored the envelope. This is not unreasonable if it is as tenuous as it has to be when the star has swollen to giant dimensions, but we have not yet addressed why this swelling actually happens. It is clear that real stars do it, and their behavior can be reproduced by models, but it is not so clear what physical mechanism dominates this process. Indeed, as was clear from the beginning of this chapter, this question is still debated (see the references quoted there for more detail).

Partly, it seems it is related to the way the opacity varies with density and opacity. Quite generally, as a star becomes more luminous, its radius increases and effective temperature decreases a little. This in itself is not enough to bring the star over to the red giant regime. As the temperature in the outer layers decreases, however, the opacity there increases quite strongly, since it is dominated by bound-free processes (the lower temperature leads to lower ionization states of the metals, which therefore can absorb photons more easily). Therefore, the luminosity cannot easily be transported anymore, and part of it is trapped, leading to further expansion. At some point, this apparently can become a runaway process, in which the envelope cools more and more, becomes more and more opaque, traps more and more of the luminosity, and expands to larger and larger radii. It only stops when the star reaches the Hayashi line, where the envelope has become almost completely convective, and energy can be transported more easily.

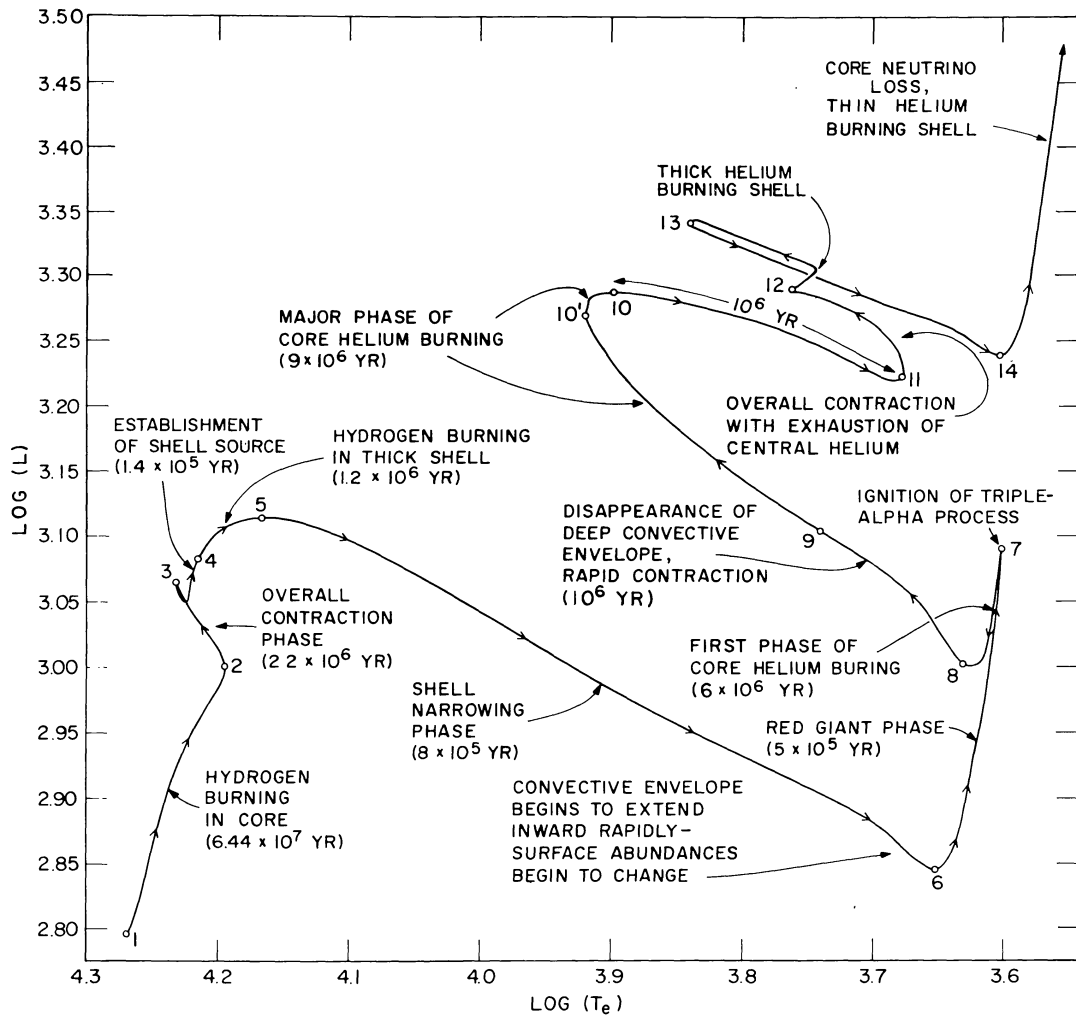
This runaway expansion may be responsible for intermediate-mass stars crossing the HR diagram very fast. Observationally, this results in a lack of stars between the main sequence and the giant branches, in the so-called *Hertzsprung gap*. When the luminosity decreases, it appears the inverse instability can happen, where the envelope heats a little, becomes less opaque, therefore shrinks a little, releasing energy which increases the temperature, etc. This deflation instability might be responsible for the blue loops seen in the evolutionary tracks of intermediate-mass stars.

### *For next time*

- Read textbook §15.1 on the fate of high mass stars, and §15.3 on core collapse (up to p. 534).



**Fig. 12.1.** (Left) Schematic evolutionary tracks in the HR diagram for stars of low, intermediate, and high mass. Heavy portions indicate phases where the evolution proceeds on a slow, nuclear timescale. Indicated are the first and second “dredge up,” phases in which the outer convection zone reaches down to layers with processed material. A third dredge-up occurs during the thermal-pulse phase, which is also indicated. Note that the luminosity at which a star leaves the AGB is a conjecture based on observed white-dwarf masses. (Bottom) Evolutionary track of a  $5 M_{\odot}$  star in detail, with important physical processes for the different phases indicated (note that the loop from point 11 to point 14 is probably spurious — this track was taken from a less accurate computation, performed several decades earlier). Both figures taken from the review of Iben (1991, ApJS 76, 55).



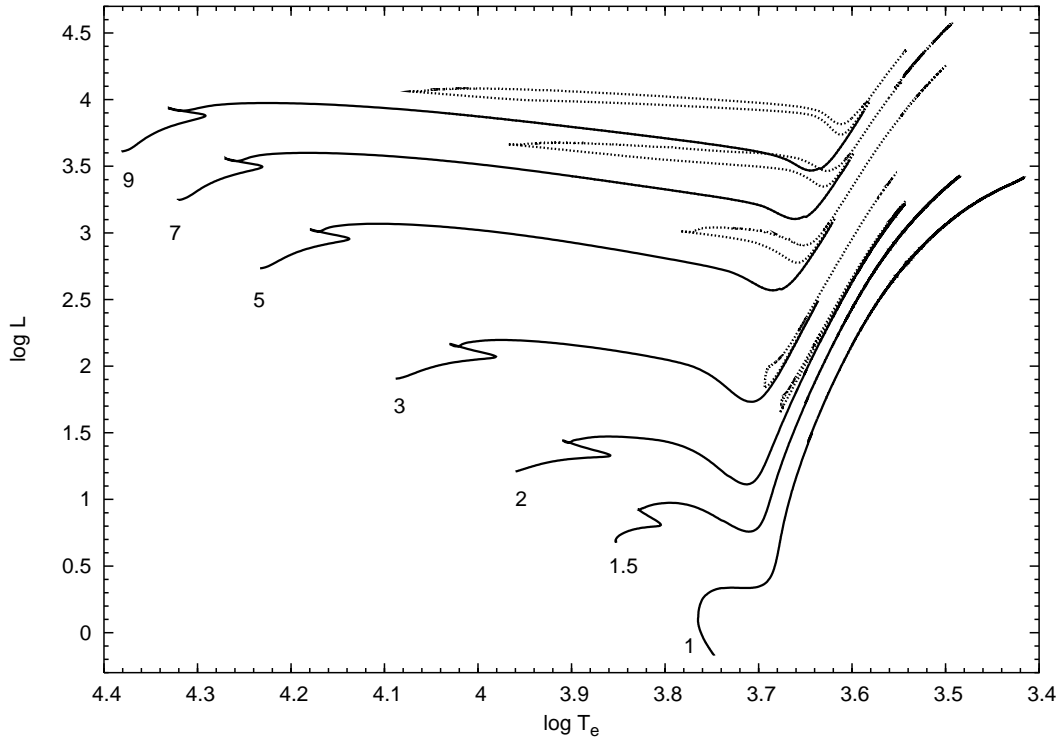


**Fig. 12.2.** Evolution of solar-metallicity stars of low and intermediate masses. *Solid lines*: evolution from the ZAMS to core helium ignition; *dotted lines*: subsequent evolution. For the 1 and 1.5  $M_{\odot}$  cases, evolution is shown only up to the beginning of the helium core flash (at the tip of the RGB). For 2–7  $M_{\odot}$  cases, evolution is shown up to the first helium shell flash (on the AGB, but *not* its tip) — the 2  $M_{\odot}$  track *includes* the helium core flash. For the 9  $M_{\odot}$  case, evolution is shown up to core carbon ignition.

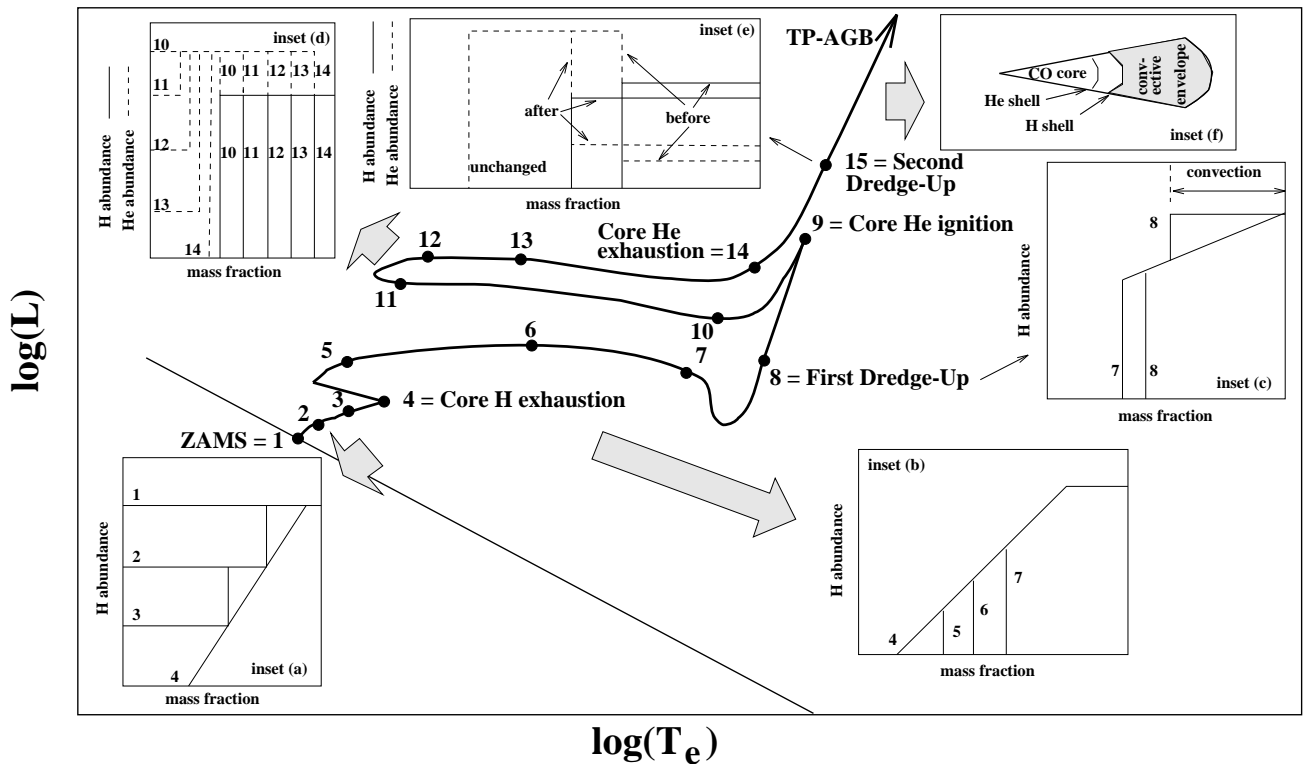


**Fig. 12.3.** Schematic evolution of a 5  $M_{\odot}$  star (from Lattanzio & Boothroyd 1995).

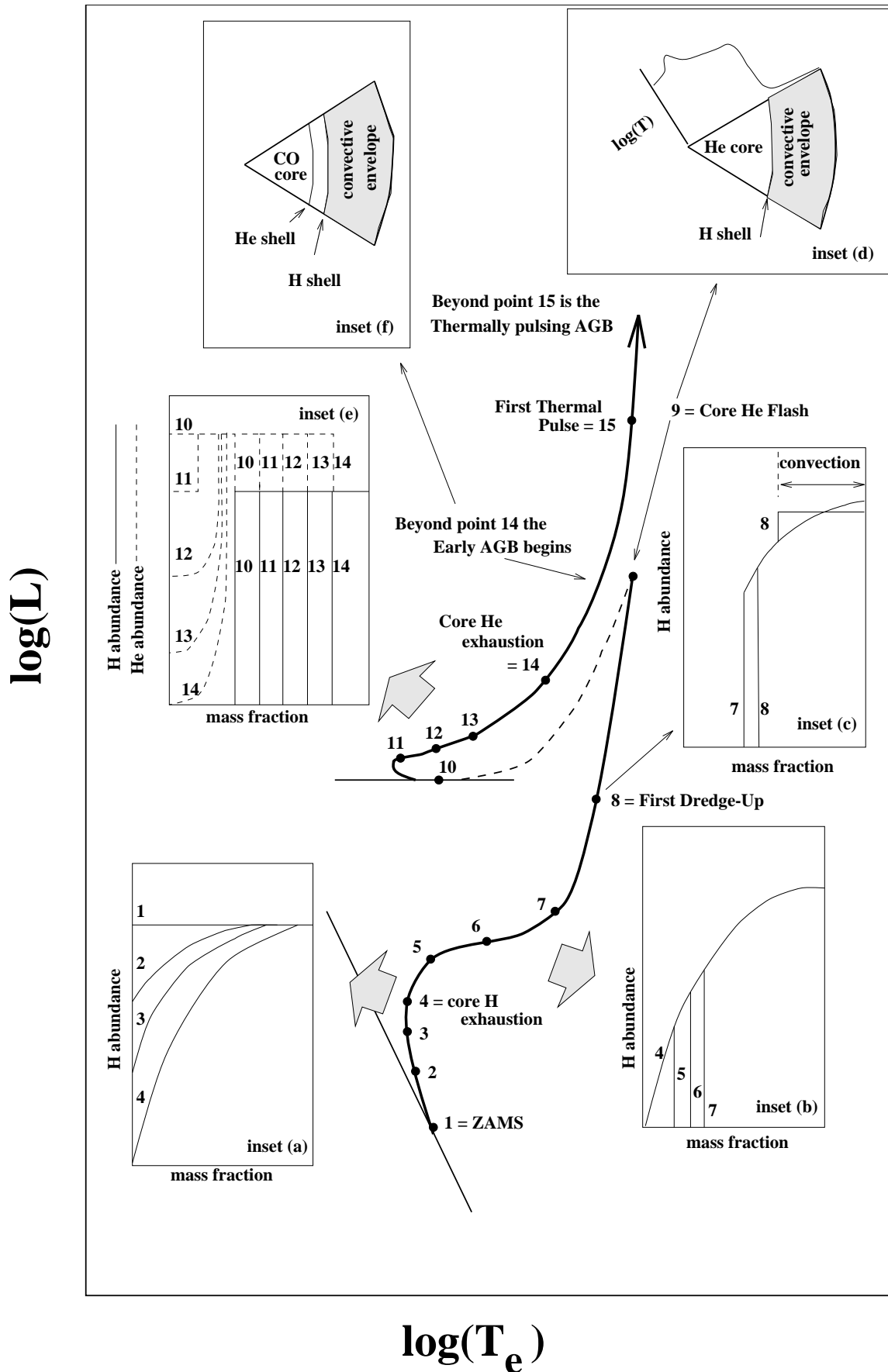
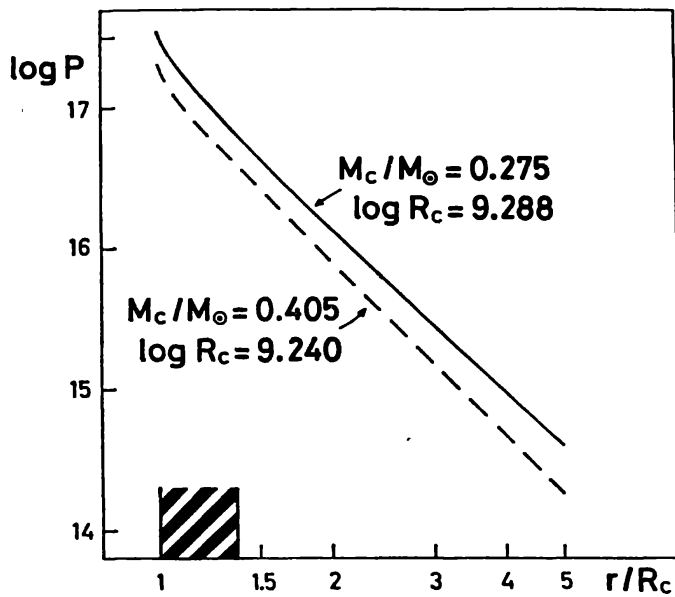
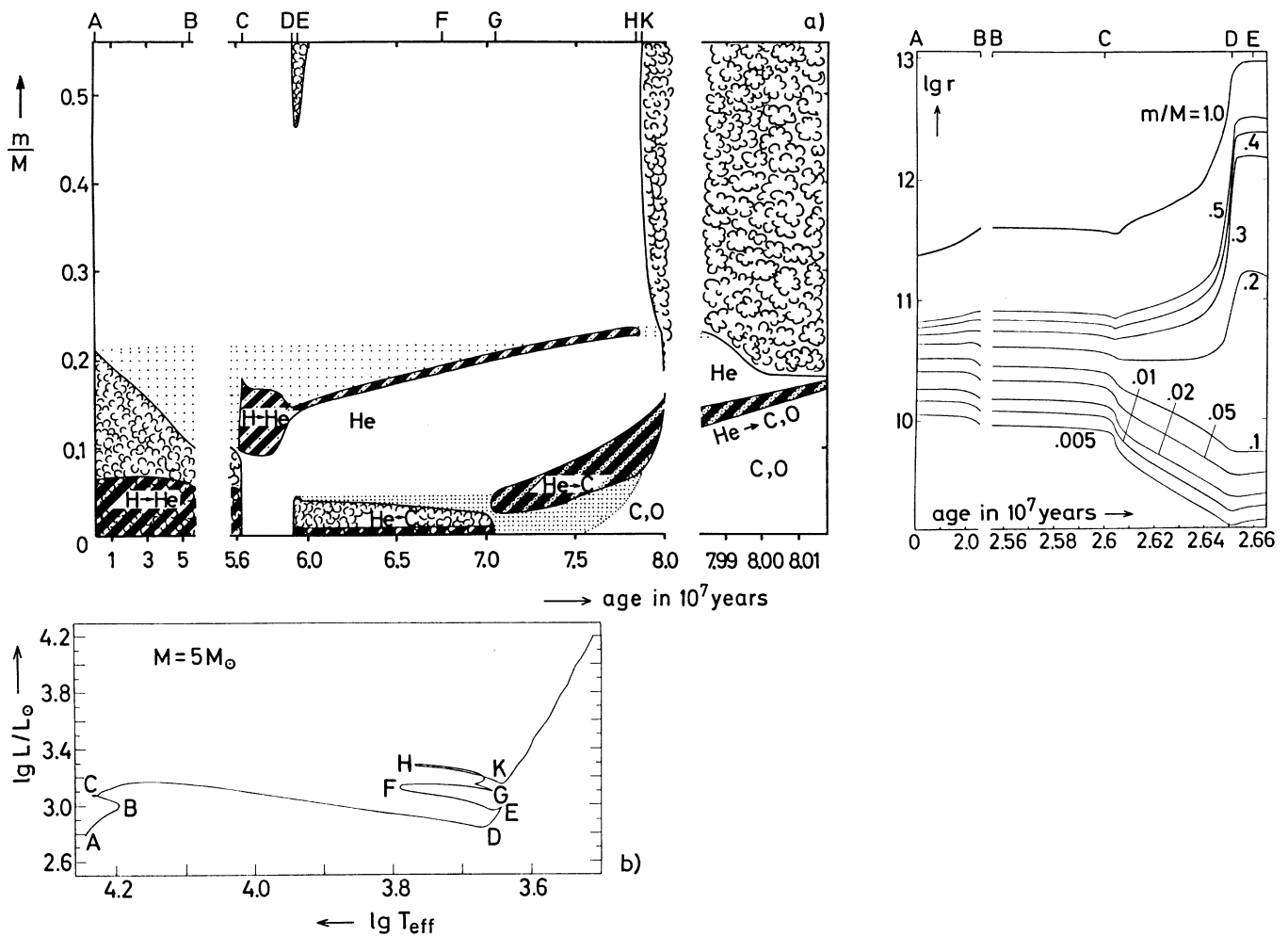


Fig. 12.4. Schematic evolution of a  $1 M_{\odot}$  star (from Lattanzio & Boothroyd 1995).



**Fig. 12.5.** Run of pressure as a function of radius in units of the core radius for two RGB models with  $M = 1.4 M_{\odot}$  but different core masses and radii. Note how similar the two curves are, apart from a constant offset (which is a function of the core properties only). The striped area indicates the extension of the burning region within the shell ( $0 < L_r < 0.99L$ ). Taken from Refsdal & Weigert (1970, A&A 6, 426).



**Fig. 12.6.** (Upper left) Interior structure of a  $5 M_{\odot}$  star during its evolution. “Clouds” indicate convective regions, heavy shading energy generation at rates  $\epsilon > 10^3 \text{ erg g}^{-1} \text{ s}^{-1}$ , and stippling variable chemical composition. (Lower left) Evolutionary track in the HRD for the same model. (Right) Radial variation of different mass shells during the evolution of a  $7 M_{\odot}$  star. The letters A, ..., E correspond to the same evolutionary phases labeled for a  $5 M_{\odot}$  star in the left-hand panels. Taken from KW, their Figs 31.2, 3.

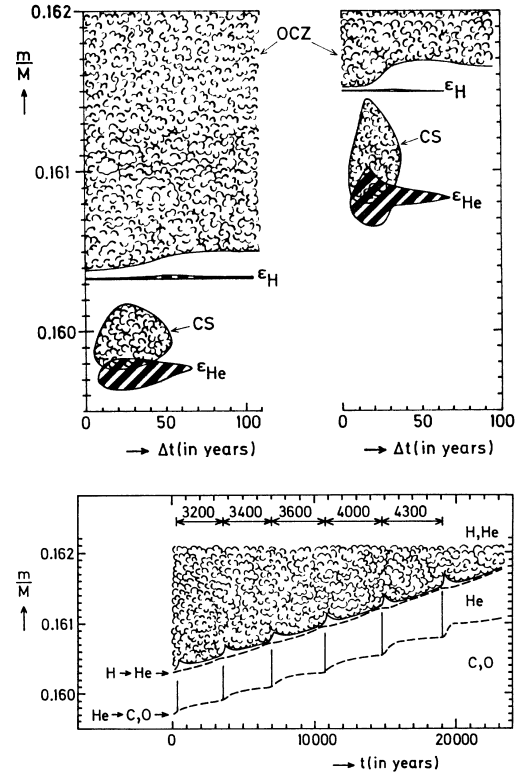
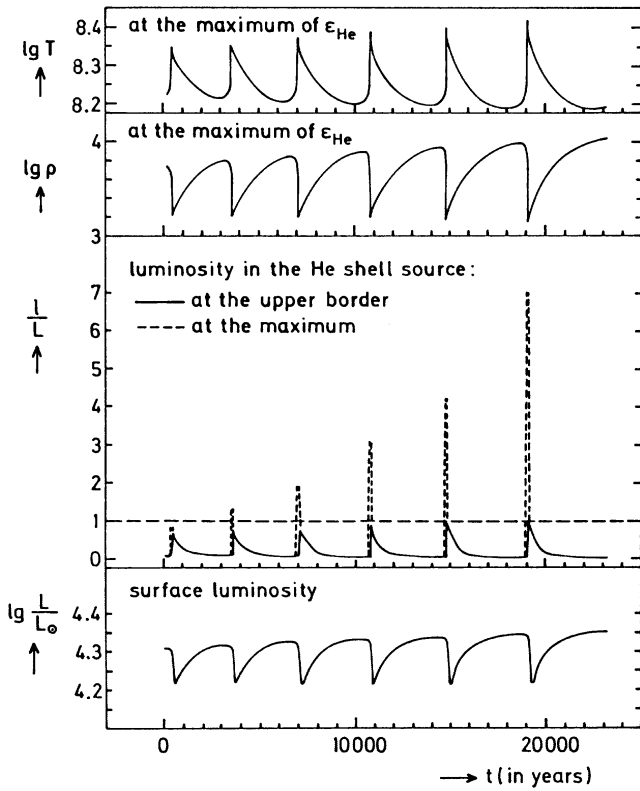


**Fig. 12.7.** Shell flashes. (Left) The four panels give the evolution of the temperature and density in the shell at the position of maximum energy generation, luminosity at that position and of the shell as a whole, and surface luminosity. (Top right) Details of the star's structure near the shell during two shell flashes. (Bottom right) Evolution of the star's structure during a series of shell flashes. Taken from KW, their Figs 33.3, 4, 5.

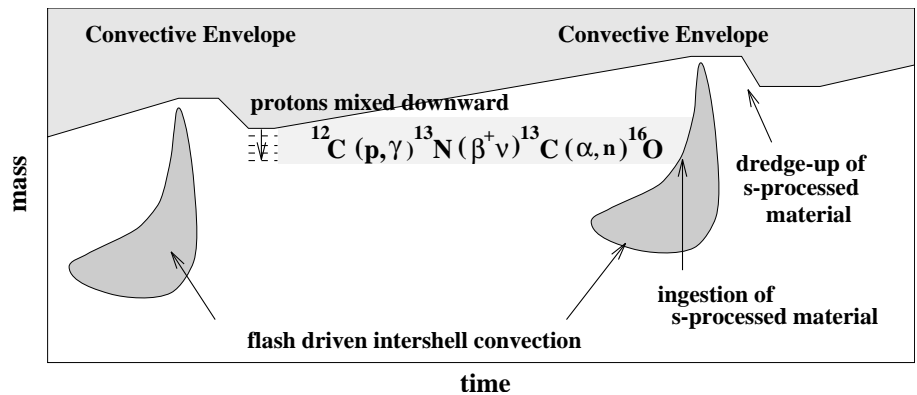
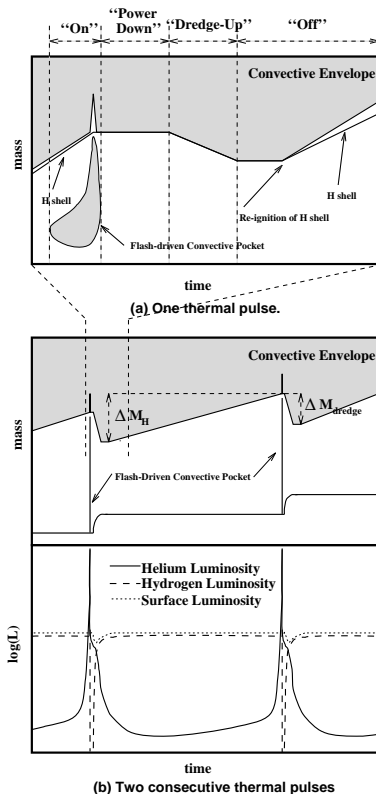


**Fig. 12.8.** (Left) Interior structure and surface, hydrogen shell, and helium shell luminosities during helium shell flashes with third dredge-up. The hydrogen shell advances by  $\Delta M_H$  between flashes, with this advance then being "set back" by  $\Delta M_{dredge}$ , the amount of mass "dredged up". (Above) Schematic of the steps yielding s-process enrichment; note that the mechanism by which protons are mixed downwards into the carbon-rich intershell region is not well understood.

### 13. The end of a star's life

Textbook: §15.1, 15.3 (up to p. 534; different emphasis)

#### *Dwindling into oblivion ...*

A very simple picture of the evolution of a star can be obtained from looking just at the changes in central density and temperature, as is done in Fig. 13.1. While a star contracts more or less homologously, and the core is not degenerate, one has  $\rho \propto R^{-3}$  and  $T \propto R^{-1}$ , from which it follows that  $T \propto \rho^{1/3}$ . This behaviour can indeed be seen in the lower left corner of the figure.

The demarcation between the regions in  $\rho, T$  space where the ideal gas law holds and where degeneracy is important, is described by a line  $T \propto \rho^{2/3}$ . Therefore, during contraction, the core of a star comes closer and closer to being degenerate. Before doing so, however, it may reach conditions sufficient to start nuclear processing, indicated by the various ignition lines in the figure. If it does not even reach hydrogen ignition, it becomes a brown dwarf.

When hydrogen is ignited, the properties can remain similar, while the star is on the main sequence. When hydrogen is exhausted, however, the core starts to contract again. For low-mass stars, we saw that the core becomes degenerate before helium is ignited. If the star does not have sufficient mass, the core cannot grow up to  $0.45 M_{\odot}$ , and helium will not be ignited; the star will dwindle, and become a helium white dwarf.<sup>4</sup>

For both low and intermediate-mass stars, the carbon-oxygen cores become degenerate after helium burning. In principle, if the star were massive enough, the core might grow sufficiently due to shell burning to ignite carbon burning. If so, the star would likely explode, leaving no remnant. In practice, however, it seems the super wind intervenes, and no carbon-oxygen cores above  $\sim 1.2 M_{\odot}$  are formed.

#### *... or going out with a bang*

For high-mass stars, the carbon-oxygen cores do not become degenerate, igniting core carbon burning instead, and these stars can continue to further burning stages as described in §8. The stages follow each other more and more rapidly, as neutrino losses become more and more important, while the energy gain from the fusion dwindles (Fig. 8.1). Some typical numbers are listed in Table 13.1. (It is *possible* that stars in a narrow mass range near  $8 M_{\odot}$  may proceed no farther than carbon burning, and end up as oxygen-neon-magnesium white dwarfs.)

While the next stage starts in the core, the burning of lighter elements will still continue in shells. As a result, the structure of a high-mass star near the end of its life becomes somewhat akin to that of an onion, in which regions with different chemical compositions are separated by burning shells (see Fig. 13.2).

When an iron core is formed, no further energy can be gained by fusion, since iron has the largest binding energy of all elements. In order to match the neutrino losses, therefore, the core has to shrink. This will cause the temperature to rise, and at  $T > 5 \cdot 10^9$  K the photons become energetic enough to break up the iron nuclei, into  $\alpha$  particles, protons and neutrons. These reactions are endothermic and thus cool the core. As a result, the pressure drops, the core shrinks

---

<sup>4</sup> Such low mass stars have not yet had time to finish their main-sequence lives even if they were formed very early on — the universe has not lived long enough. In binaries, however, somewhat more massive stars can be “stripped” of their envelopes by mass transfer onto a binary companion while they are on the red giant branch, and these can indeed leave helium white dwarfs.

**Table 13.1.** Neutrino luminosities and timescales of late burning phases

Burning stage	..... 15 $M_{\odot}$ .....		..... 25 $M_{\odot}$ .....	
	$L_{\nu}/L$ ( $L \simeq 10^4 L_{\odot}$ )	$\tau$ (yr)	$L_{\nu}/L$ ( $L \simeq 3 \cdot 10^5 L_{\odot}$ )	$\tau$ (yr)
C	1.0	$6.3 \cdot 10^3$	8.3	$1.7 \cdot 10^2$
Ne	$1.8 \cdot 10^3$	7	$6.5 \cdot 10^3$	1.2
O	$2.1 \cdot 10^4$	1.7	$1.9 \cdot 10^4$	0.51
Si	$9.2 \cdot 10^5$	0.017	$3.2 \cdot 10^6$	0.004

Taken from KW, their Table 33.1

further, more iron becomes disintegrated, etc. At the same time, neutrinos keep on removing energy. Furthermore, as the density increases, electrons are being captured by remaining heavy nuclei (leading to neutronisation, i.e., converting a proton into a neutron, with the emission of a neutrino), thus reducing the pressure further. All these processes quicken the collapse.

At first, the core collapses roughly homologously (i.e., velocity proportional to radius), but soon this would require speeds in excess of the free-fall speed in the outer region. Thus, one has an inner collapsing core, with the outer core following on the free-fall time. The latter is of order one second. The collapse of the inner core will stop only when the neutrons become degenerate, at  $\rho \gtrsim \rho_{\text{nuc}} \simeq 10^{14} \text{ g cm}^{-3}$ . The outer layers are still falling in, however, which leads to the development of a strong shock wave, which will start to move outward. At the same time, the inner core will become more massive and, since it is degenerate, smaller.

We now estimate a few quantities for the core, taking  $M \simeq 1.4 M_{\odot}$  and  $\bar{\rho} \simeq 10^{14} \text{ g cm}^{-3}$ , and, therefore,  $R \simeq 2 \times 10^6 \text{ cm}$ . For these numbers, the potential energy is roughly

$$E_{\text{pot}} \simeq \frac{GM^2}{R} \simeq 3 \times 10^{53} \text{ erg.} \quad (13.1)$$

Since the core was much larger before the collapse, we see that a couple  $10^{53}$  erg has to be liberated. We can compare this with the energy required to dissociate the iron in the core. For every nucleon,  $\epsilon_{\text{diss}} \simeq 9 \text{ MeV} \simeq 1.4 \cdot 10^{-5} \text{ erg}$  is required (see Fig. 8.1). Thus,

$$E_{\text{diss}} = \epsilon_{\text{diss}} \frac{M}{m_{\text{H}}} \simeq 2 \times 10^{52} \text{ erg} \quad (13.2)$$

which is substantially less than the total energy available. Next, compare the potential energy with the kinetic energy given to the envelope in a supernova explosion. With an envelope mass of  $10 M_{\odot}$  and a typical (observed) velocity of  $\sim 10^4 \text{ km s}^{-1}$ , the total kinetic energy is,

$$E_{\text{kin}} = \frac{1}{2} M_{\text{env}} v_{\text{env}}^2 \simeq 10^{52} \text{ erg.} \quad (13.3)$$

Thus, there is ample energy available to expel the envelope. The energy emitted in optical light is  $\sim 10^{49} \text{ erg}$ , negligible in comparison, but leads to a luminosity similar to that of an entire galaxy during the roughly one month it lasts. By far most of the energy is lost in neutrinos.

While there is enough energy to expel the envelope, it has proven very difficult to reproduce the expulsion in models. There are three effects which can help.

1. The shock. There is enough energy in the shock for expulsion, but a lot of the energy is lost as the shock goes through the relatively dense inner part of the envelope (which is still falling in).

This is because material is shock-heated to such an extent that neutrino losses and dissociation become important. From simulations, it seems only a very strong shock could cross through these layers and lead to a *prompt hydrodynamic explosion*.

2. Neutrino radiation pressure. The core is so dense that it is optically thick to neutrinos. As a result, the neutrinos have to diffuse out, and for a few seconds the core is a strong neutrino source (with  $L_\nu \simeq 10^{53} \text{ erg s}^{-1}$ ). Above the “neutrinosphere”, a fraction of the neutrinos will still be scattered, causing a radiation pressure term just like that due to photons. By equating the force due to neutrino scattering,  $f_\nu = \kappa_\nu(L_\nu/4\pi R^2 c)$ , with that due to gravity,  $f_g = GM\rho/R^2$ , one can define a neutrino equivalent of the Eddington luminosity,  $L_{\text{edd},\nu} = 4\pi GMc/\kappa_\nu$ . From calculations, it appears that the pressure due to the neutrinos in itself is insufficient to expel the outer layers, but that an explosion can be produced in combination with the shock, via strong heating and convective motion, in the so-called *delayed explosion mechanism*.
3. Thermonuclear reactions. When the shock arrives outside the original iron core, the shock heating will increase the speed of the fusion reactions in those regions dramatically. At the increased temperature, Si-burning results mostly in  $^{56}_{28}\text{Ni}$ . This is an unstable isotope, which decays to  $^{56}_{27}\text{Co}$  through  $\beta$ -decay, with a half-life time of 6.1 d.  $^{56}_{27}\text{Co}$  is unstable as well, and decays to  $^{56}_{26}\text{Fe}$  (half-life 77.7 d). These and other decay processes keep the supernova bright for a longer time.

Note that the above description of the explosion of a massive star applies to a **Type II** supernova (classified as such by virtue of possessing hydrogen lines in its spectrum). Type I supernovae show no hydrogen lines in their spectra. **Type Ia** supernovae (with a strong Si II line at 6150 Å) result from a different mechanism: the explosion of a carbon-oxygen white dwarf, which has ignited due to accretion from a binary companion. **Type Ib** supernovae (with helium lines) and **Type Ic** supernovae (with no helium lines) appear to be the explosions of massive stars, similar to those described above, but which have lost their hydrogen envelope, or even their helium envelope, by the time of their explosion.

### *Enrichment of the interstellar medium*

Supernovae are a major source of heavy elements in the interstellar medium, contributing some helium, carbon, nitrogen, oxygen, iron, and many other elements. Intermediate mass stars (and even low mass stars) contribute some heavy elements due to the mass loss that removes their envelopes, yielding mainly helium, carbon, nitrogen, and s-process elements. There are other sources as well, including novae (recurrent thermonuclear explosions on the surfaces of accreting white dwarfs in binary systems) and cosmic rays (which produce beryllium, boron, and lithium by spallation as they hit heavier nuclei such as carbon in the interstellar medium).

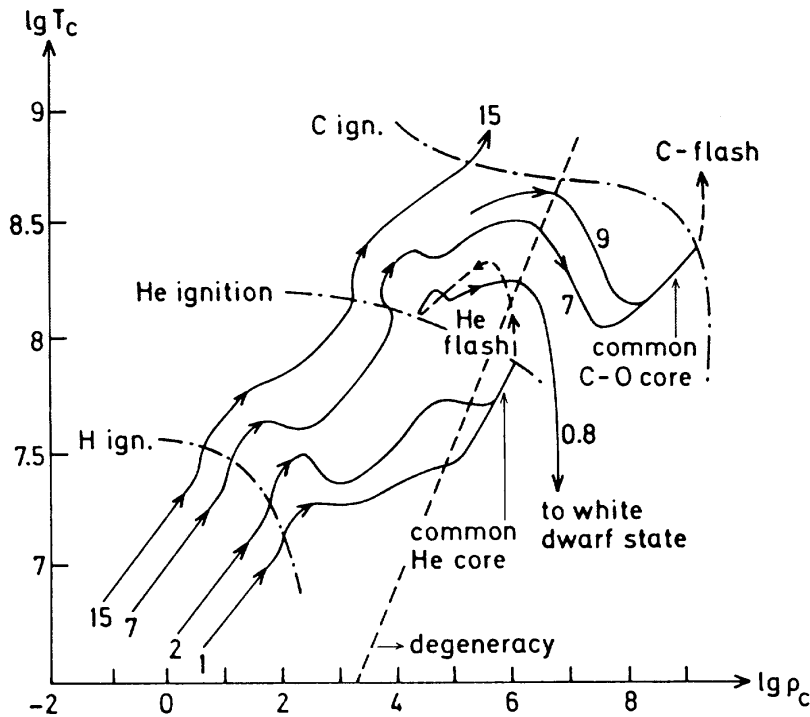


**Fig. 13.1.** Variation of central density and temperature during the course of the evolution of stars of various masses. The long-dashed line indicates the approximate limit to the right of which the core becomes degenerate. Dash-dotted lines indicate regimes where hydrogen, helium, and carbon are ignited. (Note that these earlier models showed a  $9 M_{\odot}$  star's core becoming degenerate, rather than igniting carbon burning non-degenerately. Mass loss appears to terminate AGB evolution before the C-O core reaches the "C-flash" ignition line in this diagram.) Taken from KW, their Fig. 33.6.

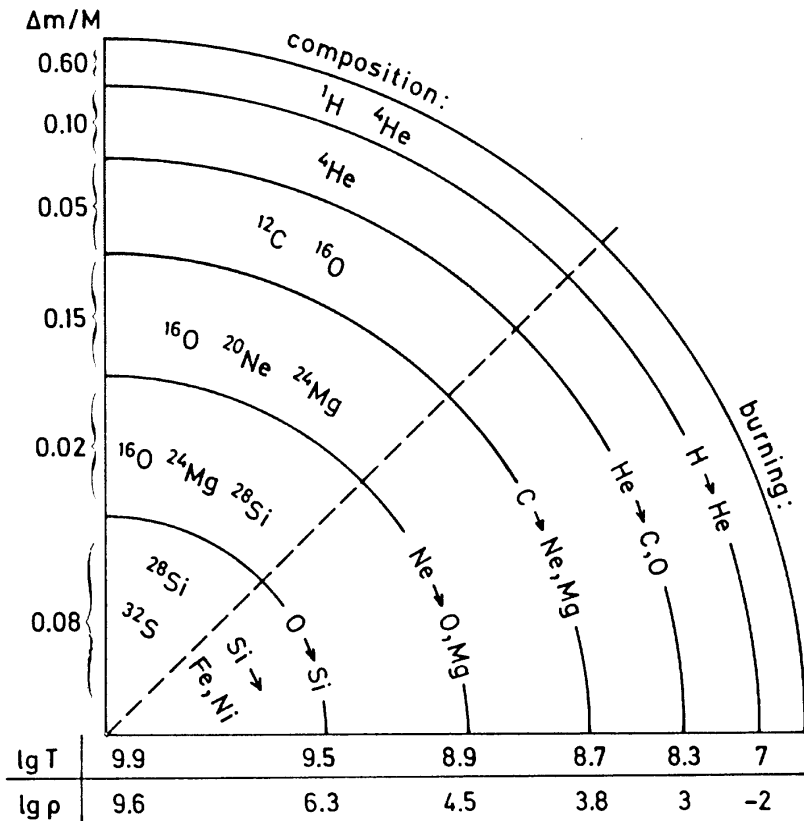


**Fig. 13.2.** "Onion-skin" structure of a massive star in the very last stages of its life (not to scale). Typical fractional masses, temperatures (K), and densities ( $\text{g cm}^{-3}$ ) are indicated along the axes. Taken from KW, their Fig. 33.1.